2009 Joint UCSD and Caltech Annual Report

Application of Waveform Cross-Correlation and Other Methods to
Refine Southern California Earthquake Data

Peter M. Shearer
Institute of Geophysics and Planetary Physics
Scripps Institution of Oceanography
U.C. San Diego
La Jolla, CA 92093-0225
pshearer@ucsd.edu

Egill Hauksson
Seismological Laboratory
California Institute of Technology
Pasadena, CA 91125
hauksson@gps.caltech.edu

Introduction

Our SCEC funded research involves the cooperation between Caltech and UCSD in earthquake seismology research in southern California. The ever-expanding waveform archive of over 400,000 local earthquake records provides an invaluable resource for seismology research that has only begun to be exploited. However, efficiently mining these data requires the development of new analysis methods, an effort that goes beyond the limited resources of individual scientists. We have coordinated our efforts and developed common tools and data products that can be used by us and other researchers to accomplish many SCEC goals.

Our collaboration has focused on a project to compute waveform cross-correlation times for all 1981–2005 events and to use these times to improve earthquake locations. The similar event clusters identified in our relocation method provide a useful set of repeatable sources for use in evaluating the temporal stability of seismic velocities across southern California. We have also applied our tools to study the 2008 Mw5.4 Chino Hills and 2010 M4.4 Pico Rivera earthquakes.

Our catalogs are available through the SCEC Data Center, and other SCEC researchers have begun to use our locations to study the fine-scale structure of seismicity in southern California. Our new SCEC activity is to test and compare existing methods for determining focal mechanisms, which has included comparing of first motion mechanisms and moment tensors. Our results will be useful in further refining the Community Fault Model (CFM) and in resolving the stress state and tectonic complexities of the southern California crust.

Technical Description of Focal Mechanisms Catalog (1981–2009)

About 15,000 focal mechanisms were selected, including only A, B, and C quality mechanisms as defined by J. Hardebeck for the previous SCSN focal mechanism catalog (1984 – 2003).

Strike-slip faulting mechanisms occur across southern California (Figure 1). They are most common along the major late Quaternary faults. Normal faulting mechanisms are dominant along the Salton Trough, and the northern end of the San Jacinto fault, and also occur in the southern Sierra Nevada and Coso regions. Thrust faulting mechanisms occur within the Transverse Ranges, beneath Banning Pass extending to the west across the Los Angles and Ventura basins. Overall, the plate boundary is characterized by strike-slip faulting with small regions of

compression and extension, which results in spatial overlaps of different types of focal mechanisms.

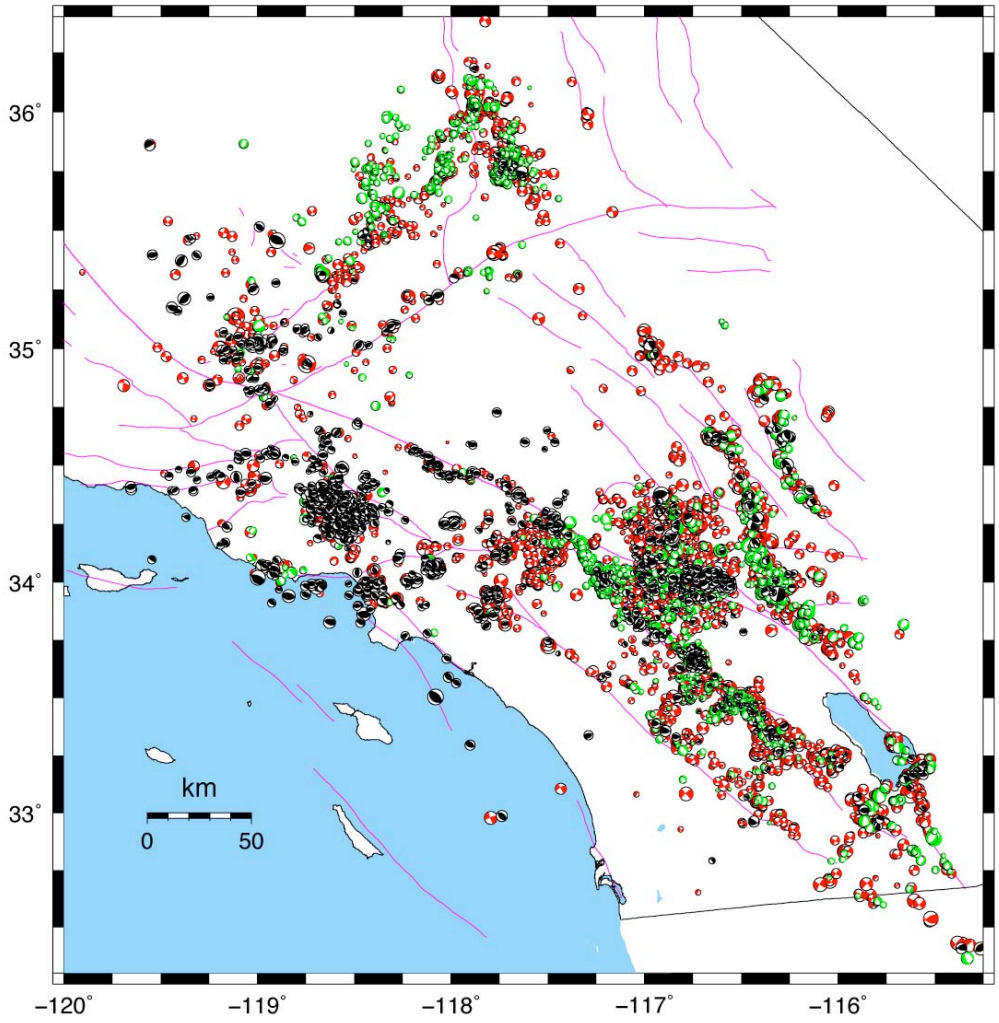

Figure 1. The ~15,000 focal mechanisms (1981 – 2009) (A, B, and C quality) selected using similar criteria as J. Hardebeck used for the previous catalog. First, the strike-slip (red) are plotted. Second, the normal (green), and thrust mechanisms (black) are plotted on top – reducing somewhat the prominence of the strike-slip events.

Analyzing Nodal Plane Errors

We have applied the HASH algorithm (*Hardebeck and Shearer,* 2002 and 2003) to determine focal mechanisms from the SCSN data set of first motion polarities. We maximize the number of mechanisms by removing azimuth, take-off angle, and distance filters. We only require more than 8 first motions for each mechanism and an azimuth gap of less than 180°. This results in 137,000 mechanisms. The algorithm provides the strike, dip, and rake for one of the two planes of each mechanism, as well as error estimates. We analyze the error estimates to look for obvious trends that would make it possible to determine filtering values to optimize the selection of reliable mechanisms.

The errors in the focal mechanisms exist because of lack of first motions, too large an azimuthal gap or take-off angle gap, poor station distribution ratio (STDR) values because the distribution

of first motions is not optimal to constrain the nodal planes; and misfit of first motions (*Kilb and Hardebeck*, 2006). The number of available first motions depends on the local density of the network, depth of the earthquake, background noise level at the time of the quake, possible over-print from an almost simultaneous earthquake, and other data availability factors.

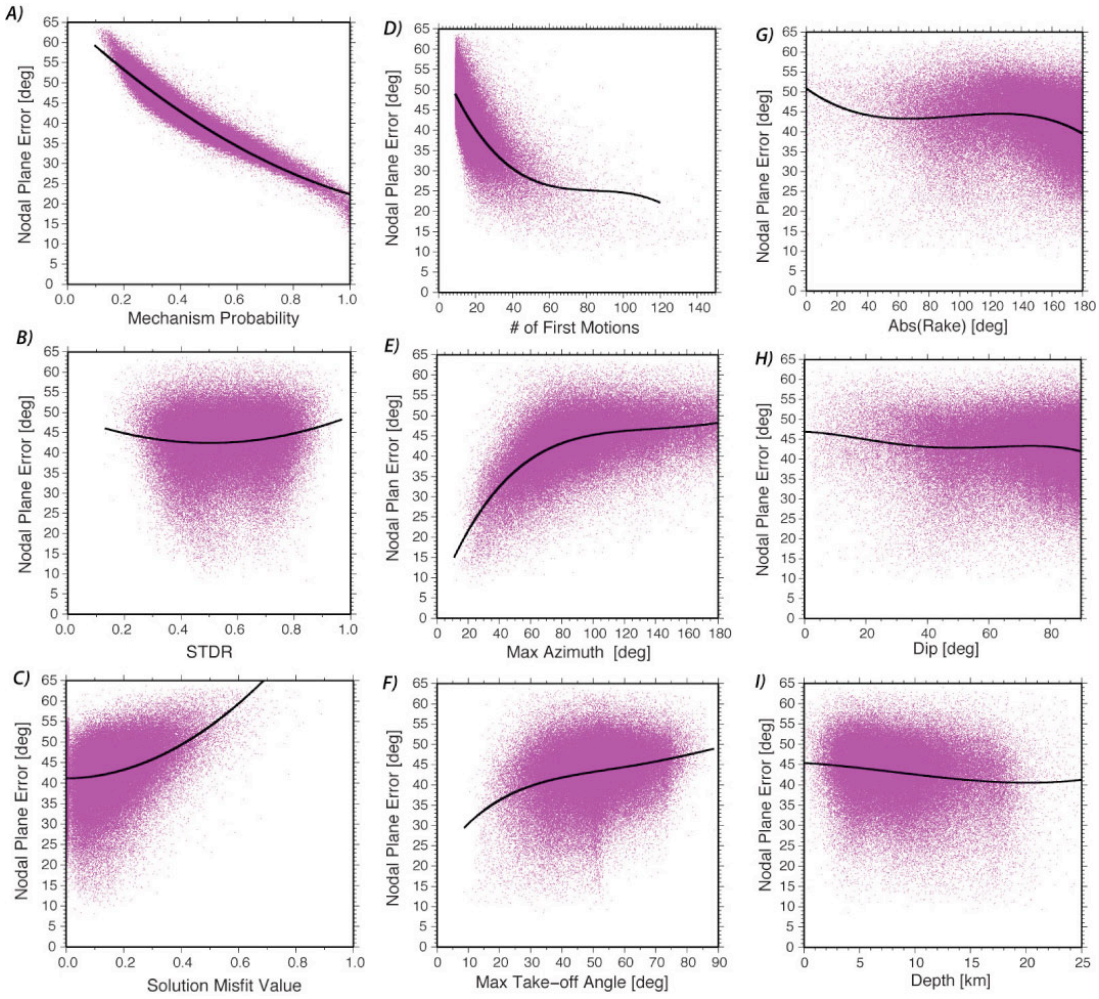

Figure 2. Nodal plane errors for 137,000 mechanisms plotted versus: (A) mechanism probability; (B) station distribution ratio (STDR); (C) solution misfit value; (D) number of first motions; (E) maximum azimuth; (F) maximum take-off angle; (G) the absolute value of the rake angle; (H) dip; and (I) focal depth. Polynomial fits are also shown.

The nodal plane errors are defined as 1-sigma fault plane uncertainties, defined as the Root-Mean-Square (RMS) angular difference of the acceptable fault planes from the preferred plane (Figure 2). The first set of parameters are measures of the quality of the mechanisms (Figure 2, A, B, & C). The mechanism probability is defined as the fraction of the acceptable solutions that exist within 30° of the preferred solutions. As shown in Figure 2A, the mechanism probability is inversely related to the nodal plane error. The station distribution ratio (STDR) represents the distribution of first motion data on the focal sphere. If the STDR is small, most of the data are close to the nodal planes. The fraction of misfit polarities also contributes to the mechanism uncertainty, where 0.0 is a perfect fit and 1.0 would be a perfect misfit. Although STDR and misfit values are often used to classify mechanisms, there are no obvious trends or clusters in STDR or misfit values that allow simple A, B, C, etc. quality type classification of the mechanisms.

In general the available first motions for each event increase with magnitude. The number of first motions depends on the local density of the network, the depth of the quake, the background noise level at the time of the quake, possible over-print from almost simultaneous earthquakes, and other data availability factors. The number of first motions does not have a simple cut-off magnitude, and in some cases good focal mechanisms can be determined successfully for very small earthquakes of M<1.0.

The parameters in Figure 2 D, E, and F show that number of first motions and azimuth gap of ~<100° matter but variations in take-off angle are not diagnostic for mechanism quality. Similarly, Figures 2 G, H, and I show that the nodal plane errors do not vary significantly with the type of mechanism or the focal depth of the event.

In summary, the nine plots in Figure 2 demonstrate that the focal mechanism quality is dependent on the number of first motions available, while more general quality parameters do not facilitate the separation of high quality mechanisms from low quality mechanisms.

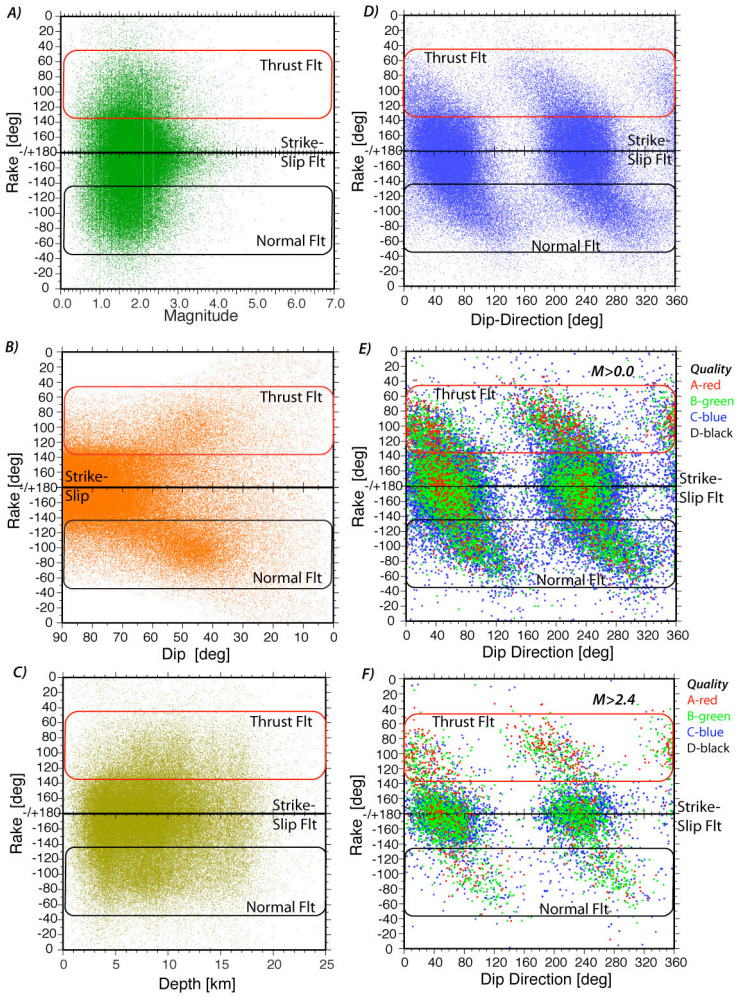

Figure 3. The rake versus (A) magnitude, (B) dip, (C) focal depth, (D) dip-direction, (E) dip-direction selected with standard filtering, and (F) dip-direction also selected with M>2.4.

Focal Mechanism Parameters

The distribution of rake values describes the types of mechanisms (Figure 3). We explore how the rake varies with magnitude, dip, and focal depth. We also compare three different data sets of rake versus dip-direction plots to investigate if there are any simple patterns that emerge as a result of applying the traditional quality filters.

The rake values of 45° to 135° are classified as thrust faulting events, -45° to -135° are normal faulting events while all other events are deemed strike-slip events. The normal events are more common than the thrust events but appear to have slightly lower average magnitudes. All other events are considered to be strike-slip. The majority of events have strike-slip faulting, which is also more common for M>3 events (Figure 3A).

This rake versus dip plot shows three distinct distributions, with strike-slip, normal, and thrust faulting. These distributions are contiguous but separate distributions (Figure 3A). Similarly, the rake versus depth plot shows that normal faulting is more common at depths between 3 and 10 km while thrust faulting is more common 3 to 5 km deeper (Figure 3B).

The rake versus dip-direction plots show all the mechanisms, only mechanisms selected by quality, and mechanisms selected by an additional magnitude constraint of M>2.4 (Figure 3 D, E, and F). The overall pattern of rakes and dip-directions remains the same, showing the 'bad' mechanisms do not introduce a particular bias into the data set.

Temporal Stability of Focal Mechanisms

The average quality of the focal mechanisms and style of faulting has remained similar from 1981 to 2009 (Figure 4). As an example, the time-series of normalized dip-direction values corresponds an average crustal deformation in the direction of N30°W, which is ~10° more northerly than the average Pacific North America plate motion. Similarly, the time-series of rake values shows ongoing strike-slip deformation with a small component of normal faulting or rake of ~ -170°. The time-series of the dip values has an average value of ~70°. All of these average values include both strike-slip and dip-slip faulting.

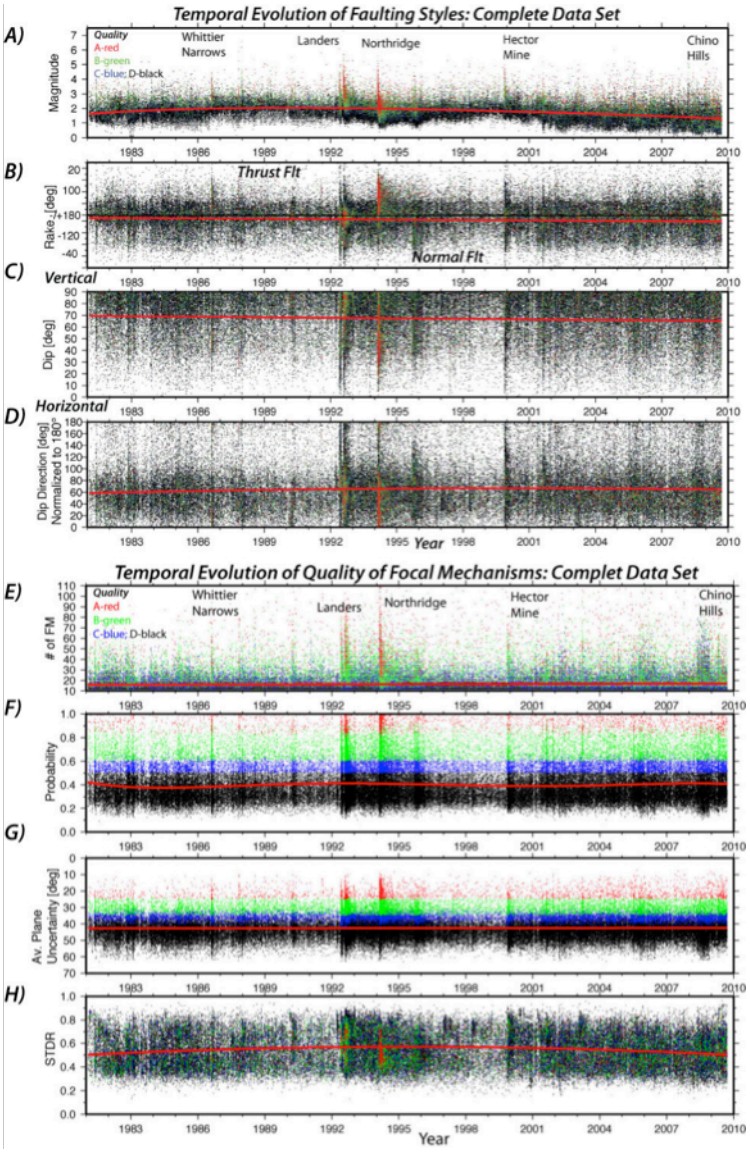

Figure 4. The temporal evolution of the faulting styles. (A) magnitude, (B) rake, (C) dip, (D) dip-direction, (E) number of first motions, (F) mechanisms probability, (G) average plane error (inverted scale), (H) station distribution ratio (STDR). The colors indicate mechanism quality, (A) red, (B) green, (C) blue, and (D) black. Curves (red) are polynomial fits.

The number of events that qualify for focal mechanism determination remained steady during the late 1980s and the 1990s but increased in the 2000s, with the addition of new digital stations to the SCSN as part of the TriNet project.

The average quality of the focal mechanisms exhibits only small variations with time. The average mechanism probability remains constant, with a broad scatter. The Average Plane Error of 40° remains constant with a broad scatter from 20° to 60°. The station distribution ratio that describes the distribution of stations on the focal sphere was higher during the 1990s. The higher station distribution ratio is more desirable for improved constraints on the focal mechanisms. These error estimates reflect how the configuration of the network has remained similar during the last 30 years, and our ability to determine focal mechanisms has remained fairly constant, except for the improvements starting in 2000. The quality of

mechanisms appears to increase temporarily at the time of major sequences. As an example, the 1994 Northridge sequence shows high quality of mechanisms for the whole sequence, but it was also located near the center of the seismic network. The temporal behavior of all the focal mechanism parameters and their errors are very similar from 1981 to 2009. Thus the tectonics of southern California has remained similar, and the predominant style of faulting changed only during major earthquake sequences.

References

Hardebeck, J.L. and P.M. Shearer, A new method for determining first-motion focal mechanisms, *Bull. Seismol. Soc. Am*, **92**, 2264–2276, 2002.

Hardebeck, J.L. and P.M. Shearer, Using S/P amplitude ratios to constrain the focal mechanisms of small earthquakes, *Bull. Seismol. Soc. Am.*, **93**, 2434–2444, 2003.

Kilb, D., and J. L. Hardebeck, Fault Parameter Constraints Using Relocated Earthquakes: A Validation of First-Motion Focal-Mechanism Data, Bull. Seism. Soc. Am., 96, No. 3, pp. 1140–1158, June 2006, doi: 10.1785/0120040239.

Recent Publications

Allmann, B. P., P. M. Shearer, and E. Hauksson, Spectral discrimination between quarry blasts and earthquakes in southern California, *Bull. Seismol. Soc. Am.*, 98, 2073-2079, 2008.

Hauksson, E., K. Felzer, D. Given, M. Giveon, S. Hough, K. Hutton, H. Kanamori, V. Sevilgen, S. Wei, and A. Yong, Preliminary Report on the 29 July 2008 Mw5.4 Chino Hills, Eastern Los Angeles Basin, California, Earthquake Sequence, *Seismo. Res. Letters*, vol. 79, p. 855-868, 2008

Hauksson, E., Spatial Separation of Large Earthquakes, Aftershocks, and Background Seismicity: Analysis of Interseismic and Coseismic Seismicity Patterns in Southern California, *Special Frank Evison Issue of Pure Appl. Geophys.*, DOI 10.1007/s00024-010-0083-3, 2010.

Hutton, L. K., J. Woessner, and E. Hauksson, Seventy-Seven Years (1932 – 2009) of Earthquake Monitoring in Southern California, *in press, Bull. Seismol. Soc. Am*, 2010.

Lin, G., P. Shearer, and E. Hauksson, A Search for Temporal Variations in Station Terms in Southern California from 1984 to 2002,*Bull. Seismol. Soc. Am.,* 98: 2118 – 2132, 2008.

Lin, G., and P. M. Shearer, Evidence for water-filled cracks in earthquake source regions, *Geophys. Res. Lett.*, **36**, L17315, doi:10.1029/2009GL039098, 2009.

Lin, G., C. H. Thurber, H. Zhang, E. Hauksson, P. M. Shearer, F. Waldhauser, T. M. Brocher and J. Hardebeck, A California statewide three-dimensional seismic velocity model from both absolute and differential times, *Bull. Seismol. Soc. Am.*, **100**, 225-240, doi: 10.1785/0120090028, 2010.